An Integrated Programmable High-Voltage Bipolar Pulser With Embedded Transmit/Receive Switch for Miniature Ultrasound Probes

Article *in* IEEE Solid-State Circuits Letters · September 2019

DOI: 10.1109/LSSC.2019.2938141

CITATIONS
7

READS
529

7 authors, including:

Mingliang Tan
Delft University of Technology
14 PUBLICATIONS **223** CITATIONS
SEE PROFILE

JAE-SUNG AN
Delft University of Technology
24 PUBLICATIONS **237** CITATIONS
SEE PROFILE

Philippe Vince
Vermon
18 PUBLICATIONS **93** CITATIONS
SEE PROFILE

Nicolas Sénégond
Vermon
36 PUBLICATIONS **216** CITATIONS
SEE PROFILE

An Integrated Programmable High-Voltage Bipolar Pulser with Embedded Transmit/Receive Switch for Miniature Ultrasound Probes

Mingliang Tan, *Student Member*, *IEEE*, Eunchul Kang, *Student Member*, *IEEE*, Jae-Sung An, *Member, IEEE*, Zu-Yao Chang, *Member*, *IEEE*, Philippe Vince, Nicolas Sénégond and Michiel A. P. Pertijs, *Senior Member, IEEE*

***Abstract*— This paper presents a compact programmable high-voltage (HV) pulser for ultrasound imaging, designed for driving capacitive micro-machined ultrasonic transducers (CMUTs) in miniature ultrasound probes. To enable bipolar return-to-zero pulsing and embedded transmit/receive switching, a compact back-to-back isolating HV switch is proposed that employs HV floating-gate drivers with only one HV MOS transistor each. The pulser can be digitally programmed to generate bipolar pulses with and without return-to-zero, with a peak-to-peak swing up to 60 V, as well as negative and positive unipolar pulses. It can generate bursts of up to 63 pulses, with a maximum pulse frequency of 9 MHz for an 18 pF transducer capacitance. Realized in TSMC 0.18 µm HV BCD technology, the pulser occupies only 0.167 mm^2. Electrical characterization results of the pulser, as well as acoustic results obtained in combination with a 7.5-MHz CMUT transducer, are presented.**

***Index Terms*— ultrasound, high-voltage bipolar pulser, back-to-back isolation, high-voltage floating-gate driver, transmit/receive switching, CMUT, BCD technology.**

I. Introduction

Ultrasound imaging is based on the transmission of acoustic pulses and the construction of an image from the resulting echo signals. In most medical imaging applications, the transducers used to transmit and receive ultrasound need to be driven with high-voltage (HV) pulses to generate sufficient pressure to obtain a high enough signal-to-noise ratio at the largest imaging depth, at which the echo signals are significantly attenuated due to propagation attenuation [1]. Since the required voltage levels (typically 10's of Volt) far exceed the levels that can be handled by standard CMOS technologies, the associated pulser circuits tend to be implemented in high-voltage BCD technologies [2, 3, 4, 5]. In smart miniature ultrasound probes, in which transmit and receive circuitry are integrated on an application-specific integrated circuit (ASIC) close to the transducer, the integration of HV pulsers is challenging due to the relatively large die size occupied by HV MOS transistors. The same applies to the transmit/receive (T/R) switch that protects the low-voltage receive circuitry from the HV pulses, which is typically also built using HV transistors. In particular, when many pulsers and T/R switches need to be combined in order to drive a transducer array in a pitch-matched fashion, die-size constraints are stringent [3, 4]

To reduce die size, pulser circuits that generate unipolar pulses have been used extensively, because they can be implemented with a smaller number of HV transistors [2]. However, compared to bipolar pulsers, unipolar pulsers generate more out-of-band energy, leading to a lower SNR for the same peak-to-peak voltage level [6]. In addition, techniques like pulse inversion and coded excitation are more difficult to apply with unipolar pulsers. Moreover, bipolar pulsers consume less power than their unipolar counterparts for the same peak-to-peak voltage level, provided return-to-zero (RZ) switching is used [7]. Therefore, there are significant advances in the use of bipolar pulsers.

This work presents a bipolar pulser with return-to-zero capability. In contrast with prior bipolar pulser designs [3], it does not require a separate T/R switch but uses the same HV transistors that realize the return-to-zero functionality for T/R switching, thus reducing the HV transistor count. The pulser is digitally programmable and can be reconfigured as a unipolar and bipolar pulser with programmable pulse width and return-to-zero time. It was designed for use with a capacitive micromachined ultrasound transducer (CMUT), but the presented techniques can equally well be applied to other transducers.

This paper is organized as follows. Section II discusses the circuit implementation of the pulser, starting with an overview of circuit topologies that can provide the bidirectional HV isolation needed for RZ switching and T/R switching, and then discussing the details of the proposed pulser. Section III describes the fabricated prototype and presents electrical and acoustical measurement results. The paper ends with a comparison to the prior art and conclusions.

II. Circuit Implementation

A. Bidirectional HV Isolation

As shown in Fig. 1, in order to generate RZ bipolar pulses, the pulser consists of a pull-up switch that drives the transducer (which is biased at a DC voltage V_{Bias} through an off-chip RC network) to a positive HV supply (HV_VDD), a pull-down switch that drives it to a negative HV supply (HV_VSS), and a RZ switch that pulls the transducer back to ground. The RZ switch needs to provide bidirectional HV isolation, in the sense that when it is off, it should be able to handle both positive and negative voltage drop. Similarly, the T/R switch, which connects the transducer to a low-noise amplifier (LNA) during echo reception, needs to provide bidirectional HV isolation during pulsing.

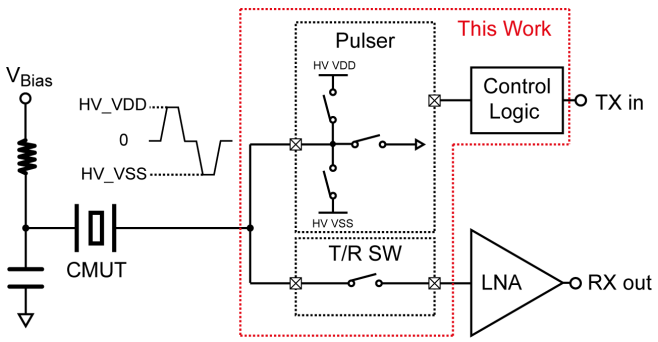

Fig. 1. Block diagram of an ultrasound front-end with a bipolar RZ pulser.

Mansucript received June. 2019

Mingliang Tan, Eunchul Kang, Jae-Sung An, Zu-Yao Chang and Michiel A. P. Pertijs are with the Electronic Instrumentation Laboratory, Delft University of Technology, 2628 CD Delft, The Netherlands. (e-mail: m.tan@tudelft.nl).

Philippe Vince and Nicolas Sénégond are with Vermon SA, 180 rue du Général Renault 37038 Tours, France.

Two technology-related limitations of the HV MOS transistors in BCD technologies, the body diode and the limited gate-oxide breakdown voltage, increase the implementation complexity of the T/R switch and RZ switch. The presence of the body diode implies that two back-to-back connected HV transistors are needed to provide bidirectional isolation. The relatively low gate-oxide breakdown voltage requires a more complicated gate-driver design compared to HV technologies with thick gate oxide.

Fig. 2 shows the eight possible back-to-back configurations of HV NMOS and PMOS transistors. The body-diode orientation in configurations (a)-(d) is such that the middle node between the transistors (V_{mid}) swings up with the positive HV pulse, while in configurations (e)-(h) it swings down with the negative HV pulse. In all configurations, at least one of the sources of the transistors swings up and/or down with the HV pulse, implying that a HV gate driver is needed that keeps the gate-source voltage below the gate-oxide breakdown limit (5.5V in our technology). To prevent this HV floating-gate driver from having to operate at both positive and negative high voltages, configurations in which the source of the left-hand transistor connects to the transducer should be avoided. Driving the source of the right-hand transistor is easier if it connects to the low-voltage circuitry rather than to V_{mid}. This leaves configurations (a) and (e) as the preferred choice, both of which are applied in parallel in our implementation.

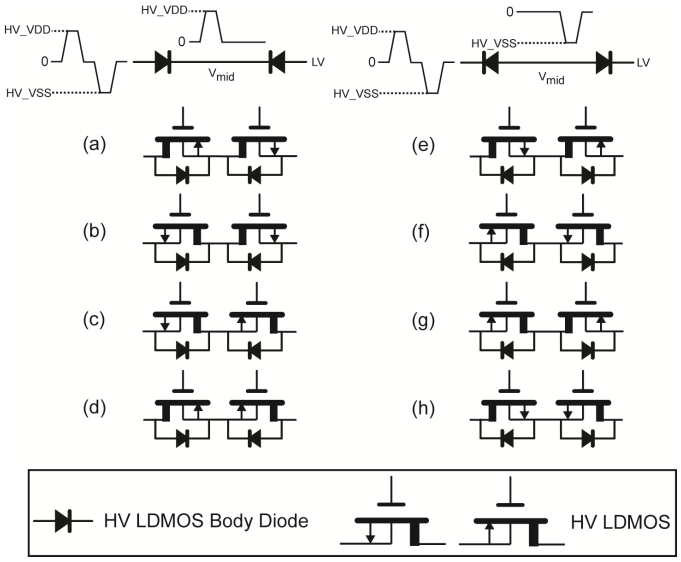

Fig. 2. Overview of HV MOS configurations that can provide back-to-back isolation.

B. Floating-Gate Driver Circuit

In previous HV switch designs [4, 5], bootstrapped gate drivers have been employed. However, they cannot be applied in an RZ switch, because they only allow the switch to be turned on when it is at ground level, while the RZ switch needs to be turned on when the pulser output is at HV_VDD or HV_VSS. Therefore, we propose a compact and energy-efficient floating-gate driver which utilizes parasitic capacitance to control the gate-source voltage and requires only one additional small HV MOS transistor.

This circuit is shown in Fig. 3, in the context of a unipolar (high-side) pulser. HV transistors MP and M1 are used to pull the transducer to HV_VDD, while M1 and M3 together form the switch configuration of Fig. 2(a) to provide the return-to-zero switching. The gate of MP is driven relative to HV_VDD using a conventional level-shifter circuit. The gate of M1 is driven by our new gate-drive approach using transistor M2.

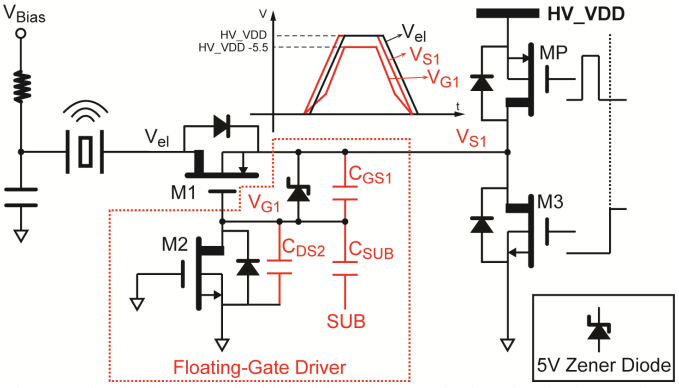

Fig. 3. Circuit diagram of a high-side pulser employing the single-transistor HV floating-gate driver circuit.

Initially, M2 is turned on to discharge the gate of M1 and then turned off to float the gate of M1. When MP is turned on, the voltage step on V_{S1} will also create a step on the gate of M1 because of the capacitive divider formed by C_{GS1} and $C_{DS2} + C_{SUB}$, where C_{SUB} is the capacitance from the gate of M1 to the substrate. By properly sizing M2 to make $C_{DS2} + C_{SUB}$ larger than C_{GS1}, V_{GS1} will increase, turning on M1 and thus allowing the transducer to be charged to HV_VDD. A Zener diode prevents V_{GS1} from exceeding the breakdown voltage. At the beginning of the RZ phase, MP is turned off and M3 is turned on, while M1 remains on. This discharges the transducer until V_{el} reaches the threshold voltage of M1 of 0.7 V (~85 times smaller than the pulse peak-to-peak amplitude), thus realizing an almost complete RZ operation. Finally, the gate of M1 is discharged by M2.

C. Embedded T/R Switch

The circuit of Fig. 3 can be extended with one additional low-voltage transistor M0 to allow it to act also as a T/R switch, as shown in Fig. 4. This transistor is placed in series with the source of M3 and is turned on during the TX phase, allowing the circuit to operate as before and preventing any feedthrough of the HV pulse from reaching the RX circuitry. Although M0 will increase the total series resistance for the RZ phase, it can be sized to have a low on-resistance compared to that of M1 and M3 without significantly affecting the total die area since it is an LV MOS transistor.

During the RX phase, when the pulser output, V_{S1}, and V_{G1} are at the ground level, M1 is turned on through M2, M3 is also turned on and M0 is turned off so that the received echo signal can pass through M1 and M3 to the LV receive circuitry. Turning on M1 through M2 requires the source of M2 to be -5 V, which is realized using a simple low-voltage charge-pump-based level shifter. Thus, only 4 HV transistors are used to implement HV pull-up, return-to-zero, and T/R switch functionality.

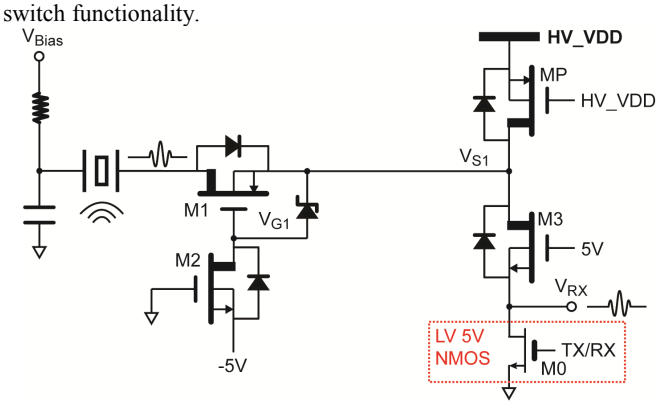

Fig. 4. Circuit diagram of the high-side pulser with embedded T/R switch.

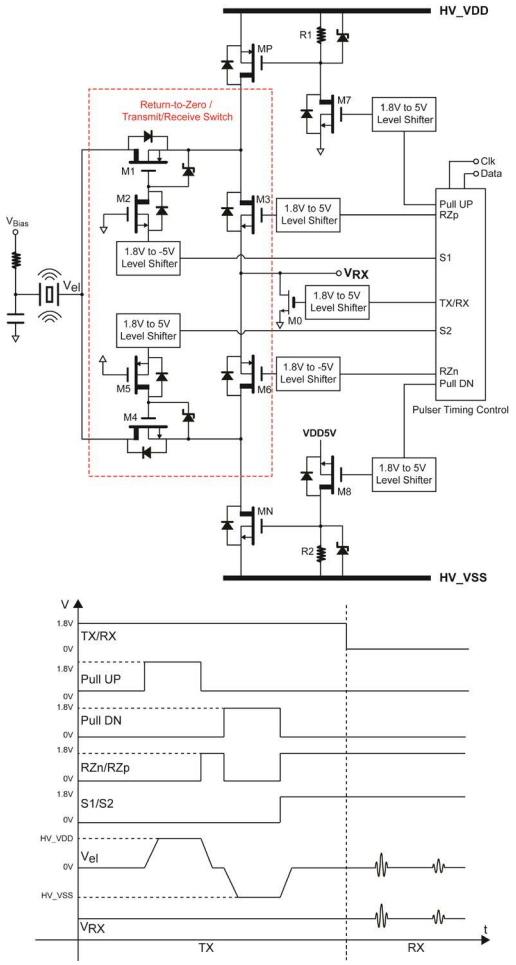

Fig. 5. Circuit diagram of the complete bipolar pulser with embedded T/R switch and the associated timing diagram.

D. Complete Pulser Implementation

To realize a complete bipolar pulser, the high-side circuit of Fig. 4 is combined with a complementary low-side version. Fig. 5 shows the resulting circuit, including the various level-shifters and the associated timing diagram. During the TX phase, M2 and M5 are turned off to float the gate of M1 and M4. Pulling up the pulser output from ground to HV_VDD and pulling down the output from HV_VDD to ground (RZ phase) are done by turning on MP and M3, respectively, as discussed in Section II.B. The same concept is applied in the complementary low-side pulser for the transition from ground to HV_VSS and HV_VSS to ground, by turning on MN and M6, respectively. After the TX phase, the two sets of RZ switches (M1, M3) and (M4, M6) are turned on in parallel to serve as a T/R switch, reducing the on-resistance (and the associated noise) by 2x, and saving substantial area compared to a separate T/R switch.

The timing logic that generates the switch control signals has been made digitally programmable via a 200 MHz SPI interface to provide the following operating modes: A) bipolar RZ pulsing as shown in the timing diagram of Fig. 5; B) bipolar non-RZ pulsing (by setting the RZ time to 0); C) unipolar pulsing (by setting the pull-up time or the pull-down time to 0). Moreover, the width of the pulses can be defined (in terms of cycles of a 200 MHz clock) to enable pulse-width programming, allowing the pulser to be used at different frequencies.

III. Experimental Results

A prototype chip including the proposed HV pulser with embedded T/R switch and an LNA has been fabricated in TSMC 180 nm HV BCD technology. Fig. 6 shows a die micrograph of the pulser. It occupies an area of 410 µm × 408 µm, of which 25% is occupied by the digital control circuitry. In addition to the HV supplies, the chip requires a 1.8 V and 5 V supply for the control logic and level shifters. Its power consumption strongly depends on the operating mode and is dominated by the dynamic power consumed in driving the transducer capacitance.

The prototype has been electrically characterized with a 18 pF capacitive load mimicking the transducer capacitance. Fig. 7 shows the measured output voltage for both unipolar and bipolar pulsing with various pulse-timing configurations, demonstrating the programmability of the pulser.

To demonstrate the functionality of the pulser in combination with an actual ultrasound transducer, measurements have been performed in which the pulser provides ±30 V pulses to a 7.5-MHz CMUT transducer with a capacitance of approximately 18 pF. The transducer was immersed in water and the pressure at 20 mm from its surface was measured using a hydrophone. The measured transient waveform of the acoustic pressure, shown in Fig. 8, is in good agreement with expectations. The measured peak-to-peak pressure of 18 kPa is in line with the pulse amplitude and the transmit efficiency of the transducer.

To demonstrate the embedded T/R switching capability of the pulser, a pulse-echo experiment has been performed in which the echo from a plate reflector is passed by the pulser to an on-chip LNA (a trans-impedance amplifier with a gain of 71.6 dBΩ and a bandwidth of 20 MHz), the output of which is captured using an oscilloscope. The result is shown in Fig. 9.

Table I compares the presented pulser and floating-gate driver with the prior art. In contrast with earlier pulsers [3, 8], this work provides embedded T/R switch functionality without increasing the number of HV transistors. Note that an area comparison is somewhat arbitrary, given the different pulser specifications and given that [3] uses HV SOI technology with smaller lateral dimensions for HV isolation than the junction-isolated technology used in this work. We expect our proposed pulser topology is equally applicable in such technology and would provide an area benefit when optimized for the much smaller matrix transducer elements used in [3]. Moreover, the floating-gate driver requires fewer HV components than those used in earlier HV switches [4, 5].

IV. Conclusions

This paper has presented a compact HV pulser design for ultrasound imaging applications. It includes a return-to-zero switch that has been constructed such that it can also serve as T/R switch. A new floating-gate driver that uses only a single HV transistor provides level-shifting functionality to turn on and off the MOS transistors in the switch. Thus, the number of HV transistors and passive components required is reduced. Electrical and acoustical experimental results have been presented that demonstrate the functionality and programmability of the pulser.

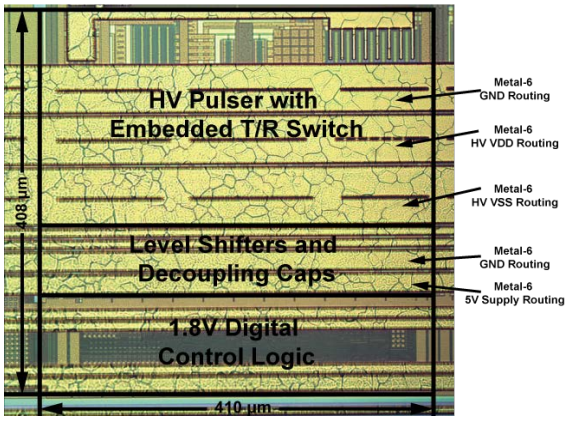

Fig. 6. Die micrograph.

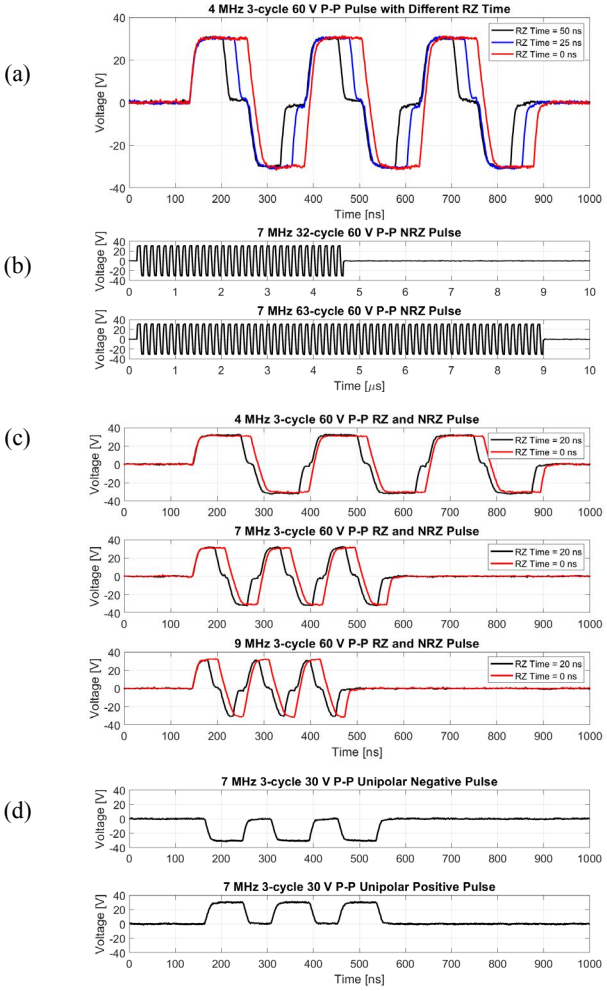

Fig. 7. Measured transient output waveforms when driving an 18 pF capacitive load with (a) 4 MHz 3-cycle 60 V pulses with RZ time of 0ns, 25ns and 50ns; (b) 7 MHz 32 and 63-cycle 60 V NRZ pulses; (c) 4 MHz,7 MHz and 9 MHz 60 V NRZ and RZ pulses; (d) 7 MHz 3-cycle 30 V unipolar negative and positive pulses.

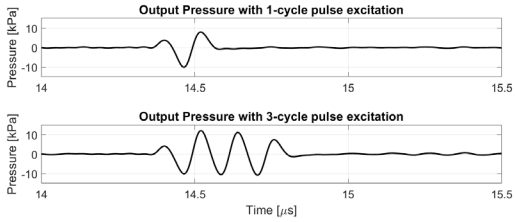

Fig. 8. Acoustic pressure generated by a CMUT transducer driven by 1-cycle and 3-cycle ±30V pulses at 7 MHz, measured in water using a hydrophone at 20 mm from the transducer surface.

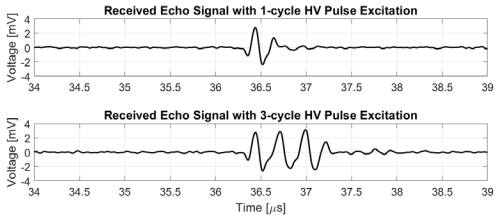

Fig. 9. Measured echo signal recorded through the embedded T/R switch and an on-chip LNA, with 1-cycle and 3-cycle HV pulse excitation.

TABLE I. COMPARISON WITH THE PRIOR ART

HV 3-level Pulser			
	This Work	ISSCC'17 [3]	JSSC'13 [8]
Technology	**TSMC 180nm HV BCD**	XFAB 180nm HV SOI	TSMC 180nm HV CMOS[a]
T/R embedded	**Yes**	No	No
Bipolar pulse	**Yes**	Yes	No
# HV MOS[b]	**10**	10 [c]	10 [c]
# HV diodes	**0**	2	0
Max output	**60 V_{pp}**	138 V_{pp}	30 V_{pp}
Pulse freq.	**9 MHz @ 18pF**	2 MHz	3.3 MHz @ 40pF
Area	**0.167 mm^2**	0.09 mm^2 [d]	0.33 mm^2 [d]
Floating-Gate Driver			
	This Work	ESSCIRC'18 [5]	JSSC'18 [4]
Technology	**TSMC 180nm HV BCD**	N/A	TSMC 180nm HV BCD
Application	**RZ & T/R switch**	HV switch (bipolar)	HV switch (unipolar)
# HV MOS	**1**	3	1
# HV diodes	**0**	3	0
# Passives[e]	**1**	6	4

a) Gate-oxide can handle 30 V swing. b) Including HV MOS in level shifters c) excluding HV transistors in T/R switch. d) Area for RX circuitry also included. e) Capacitors, resistors and Zener diodes

ACKNOWLEDGMENT

This work is supported by ULIMPIA, a labeled PENTA project endorsed by EUREKA under PENTA cluster number E!9911.

REFERENCES

[1] R. Wodnicki, B. Haider and K. E. Thomenius, "Electronics for Diagnostic Ultrasound," in *Medical Imaging: Principles, Detectors and Electronics,* K. Iniewski, Ed., New Jersey: Wiley, 2009, pp. 127-164.

[2] G. Gurun et al., "Single-Chip CMUT-on-CMOS Front-End System for Real-Time Volumetric IVUS and ICE Imaging," *IEEE Trans. Ultrason. Ferroelectr. Freq. Control,* vol. 61, no. 2, pp. 239-250, Feb 2014.

[3] Y. Katsube et al., "Single-chip 3072ch 2D array IC with RX analog and all-digital TX beamformer for 3D ultrasound imaging," in *IEEE Int. Solid-State Circuits Conf. (ISSCC) Dig. Tech. Papers*, Feb. 2017,pp. 458–459.

[4] E. Kang et al., "A reconfigurable ultrasound transceiver ASIC with 24 × 40 elements for 3D carotid artery imaging," *IEEE J. Solid-State Circuits*, vol. 53, no. 7, pp. 2065–2075, Jul. 2018.

[5] G. Ricotti and V. Bottarel, "HV Floating Switch Matrix with Parachute Safety Driving for 3D Echography Systems," in *Proc. Eur. Solid-State Circuits Conf. (ESSCIRC)*, Sep. 2018, pp. 271–273.

[6] W. Qiu, Y. Yu, F. K. Tsang, and L. Sun, "A multifunctional, reconfigurable pulse generator for high-frequency ultrasound imaging," *IEEE Trans. Ultrason. Ferroelectr. Freq. Control*, vol. 59, no. 7, pp. 1558–1567, Jul. 2012.

[7] L. Svensson and J. Koller, "Driving a capacitive load without dissipating fCV2," in *IEEE Symp. Low Power Electron. Dig. Tech. Papers*, 1994, pp. 100–101.

[8] K. Chen, H.-S. Lee, A. P. Chandrakasan, and C. G. Sodini, "Ultrasonic imaging transceiver design for CMUT: A three-level 30-Vpp pulse-shaping pulser with improved efficiency and a noise-optimized receiver," *IEEE J. Solid-State Circuits*, vol. 48, no. 11, pp. 2734–2745, Nov. 2013.